Accepted Manuscript – posprint version

Kovačević, B., Barić, D., Babić, D., Bilić, L., Hanževački, M., Sandala, G. M., … Smith, D. M. (2018). Computational tale of two enzymes: Glycerol dehydration with or without b $_{12}$. *Journal of the American Chemical Society*, *140*(27), 8487–8496. https://doi.org/10.1021/jacs.8b03109

A Computational Tale of Two Enzymes: Glycerol Dehydration With or Without B_{12}

Borislav Kovačević,[†] Danijela Barić,[†] Darko Babić,[†] Luka Bilić,[†] Marko Hanževački,[†] Gregory M. Sandala,[‡] Leo Radom,[§] and David M. Smith[†,*]

[†] Department of Physical Chemistry, Ruđer Bošković Institute, 10000 Zagreb, Croatia
[‡] Department of Chemistry and Biochemistry, Mount Allison University, Sackville, New Brunswick E4L 1G8, Canada
[§] School of Chemistry, University of Sydney, Sydney, NSW 2006, Australia

david.smith@irb.hr

Supporting Information Placeholder

ABSTRACT: We present a series of QM/MM calculations aimed at understanding the mechanism of the biological dehydration of glycerol. Strikingly and unusually, this process is catalyzed by two different radical enzymes, one of which is a coenzyme-B_{12}-*dependent* enzyme and the other which is a coenzyme-B_{12}-*independent* enzyme. We show that glycerol dehydration in the presence of the coenzyme-B_{12}-dependent enzyme proceeds via a 1,2-OH shift, which benefits from a significant catalytic reduction in the barrier. In contrast, the same reaction in the presence of the coenzyme-B_{12}-independent enzyme is unlikely to involve the 1,2-OH shift; instead, a strong preference for direct loss of water from a radical intermediate is indicated. We show that this preference and, ultimately the evolution of such enzymes, is strongly linked with the reactivities of the species responsible for abstracting a hydrogen atom from the substrate. It appears that the hydrogen re-abstraction step involving the product-related radical is fundamental to the mechanistic preference. The unconventional 1,2-OH shift seems to be required to generate a product-related radical of sufficient reactivity to cleave the relatively inactive C–H bond arising from the B_{12} cofactor. In the absence of B_{12}, it is the relatively weak S–H bond of a cysteine residue that must be homolyzed. Such a transformation is much less demanding and its inclusion apparently enables a simpler overall dehydration mechanism.

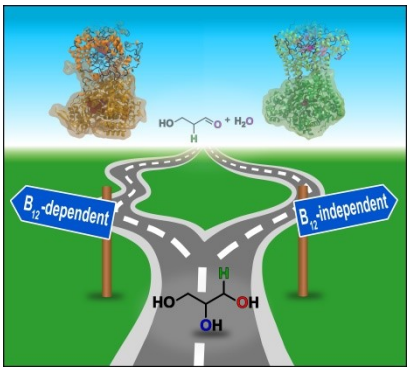

INTRODUCTION

The biological dehydration of glycerol (**1**) to 3-hydroxypropionaldehyde (**2**, 3-HPA) is an important step in the glycerol degradation pathway of certain microorganisms:[1]

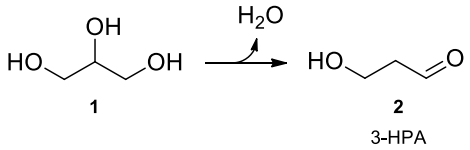

(1)

The reaction requires catalysis from a glycerol dehydratase enzyme (GDH: EC 4.2.1.30).[2] Frequently, the 3-HPA product undergoes hydrogenation, catalyzed by a 1,3-propanediol oxydoreductase enzyme (PDOR: EC 1.1.1.202), to produce 1,3-propanediol (1,3-PD),[3] which is not further metabolized. In species such as *Citrobacter freundii* or *Klebsiella oxytoca* (formerly *K. pneumoniae*), efficient glycerol degradation enables the organism to grow on glycerol as the sole carbon and energy source.[4] For *Lactobacillus brevis* and *L. buchneri*, however, additional carbon sources are required.[5]

In recent years, glycerol dehydration has received increasing attention in the context of industrial biotechnology.[6] This is primarily because glycerol is a major byproduct of biodiesel[7] and bioethanol[8] production. The increase in production of these biofuels is quickly leading to an oversupply of glycerol, and thus determining ways in which this byproduct can be usefully harnessed is becoming paramount.[9,10]

The initial product of glycerol dehydration, 3-HPA, has seen widespread use as a broad-spectrum antimicrobial agent (also known as reuterin) in food preservation.[11] While the accumulation of 3-HPA from glycerol dehydration during wine production has been linked to the presence of toxic and bitter acrolein,[12] this same transformation means that 3-HPA can be considered as a viable precursor for widely applicable acrolein-based chemicals like acrylic acid and acrylamide.[13] However, the direct use of 3-HPA is somewhat limited by difficulties in its isolation,[11] which are currently being addressed.[13]

As GDH and PDOR are most frequently co-expressed, 1,3-PD constitutes a more easily accessible glycerol derivative than 3-HPA. At the same time, 1,3-PD is a valuable chemical used to manufacture, for example, polyesters, polyethers,

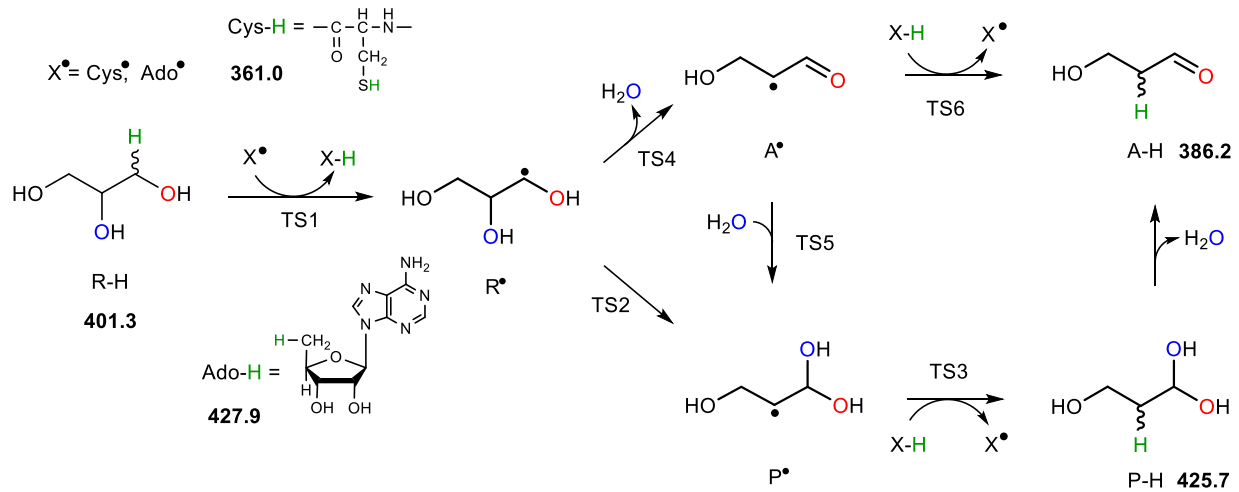

Figure 1. Possible mechanisms for glycerol dehydration following radical activation by either Ado• (B_{12}-**d**GDH) or Cys• (B_{12}-**i**GDH). The numbers in bold type depict the calculated bond dissociation enthalpies (at 298.15 K in kJ mol^{-1}) for the relevant X–H →X• + H• bond cleavage reactions. See Computational Details.

polyurethanes[14] and, in particular, the versatile polytrimethylene terephthalate.[15] 1,3-PD has also found use in coatings, solvents, and antifreezes.[16] For this reason, and because standard chemical methods for the industrial production of 1,3-PD suffer from low selectivity and contamination with impurities,[17] the microbial conversion of glycerol to 1,3-PD via 3-HPA has received significant attention in recent years.[6,9,10,14,15,18] From a biotechnological perspective, the more difficult of the two steps from glycerol to 1,3-PD is the glycerol dehydration step shown in reaction (1). The majority of metabolically engineered microbial processes established for this conversion[10,19] utilize a GDH enzyme dependent on coenzyme B_{12} (B_{12}-**d**GDH).

B_{12}-**d**GDH shares significant sequence homology with an isofunctional enzyme known as diol dehydratase (DDH: EC 4.2.1.28, hereinafter referred to as B_{12}-**d**DDH),[3] which can also dehydrate glycerol, albeit less efficiently than B_{12}-**d**GDH.[20] In addition to the B_{12} cofactor, both enzymes require monovalent cations (such as K^+),[20] although the details of such requirements differ between the two enzymes.[21] Elegant recent work by Yoshizawa and coworkers has indicated that B_{12}-**d**DDH also requires Ca^{2+} in its substrate binding pocket.[22] We are, however, not aware of any similar study to date for B_{12}-**d**GDH so the nature of the active-site cation in this case remains to be definitively determined. The X-ray crystal structure of the recombinant B_{12}-**d**GDH of *K. oxytoca* has been solved (indicating K^+ as the monovalent cation),[23] revealing also a strong structural similarity to B_{12}-**d**DDH.[24]

Both B_{12}-**d**DDH and B_{12}-**d**GDH are thought to follow the generalized mechanism for coenzyme-B_{12}-dependent reactions, whereby the unique Co–C bond of coenzyme B_{12} is cleaved homolytically to produce cob(II)alamin and the highly reactive 5'-deoxyadenosyl radical (Ado•).[20,25,26,27] Substrate catalysis (Figure 1) begins with the removal of one of the substrate (R-H) hydrogen atoms by Ado• to yield 5'-deoxyadenosine (Ado–H) and a substrate-derived radical (R•). This radical could conceivably eliminate H_2O to form an aldehyde-related radical (A•), whose subsequent quenching by Ado–H would form the product aldehyde (A-H) directly. Such a mechanism would, however, not be consistent with experiments performed with B_{12}-**d**DDH and ^{18}O-labeled propane-1,2-diols,[28] which indicate that the eliminated oxygen may originate from either the 1- (red) or the 2- (blue) position (Figure 1).[29] For this reason, it has been proposed that the substrate-derived radical (R•) undergoes a rearrangement to a product-related radical (P•), whose recapture of an H-atom from Ado–H would regenerate Ado• and form the 1,1-diol product (P-H).[30] Dehydration of the latter species can then yield the product aldehyde (A-H) in a manner consistent with the aforementioned labeling experiments.

Because the radical intermediates depicted in Figure 1 are highly reactive and difficult to observe, many of the mechanistic studies on B_{12}-**d**GDH and B_{12}-**d**DDH, which will be discussed in more detail in the Results and Discussion section, have been performed using EPR spectroscopy,[31,32] computational techniques,[22,29,33,34] site-directed mutagenesis,[35] or a combination of the latter two approaches.[36]

For many years, the B_{12}-dependent dehydratases (B_{12}-**d**DDH and B_{12}-**d**GDH) were thought to be the only enzymes capable of catalyzing the transformation shown in reaction (1). In 2003, however, a coenzyme-B_{12}-independent form of GDH (B_{12}-**i**GDH) from *Clostridium butyricum* was isolated, described,[37] and characterized (including the resolution of the X-ray crystal structure).[38] Although B_{12}-**d**GDH and B_{12}-**i**GDH are isofunctional, they share very little sequence homology and are structurally very distinct.[6] B_{12}-**i**GDH is actually a glycyl-radical enzyme[38] and exhibits significant sequence and structural similarity with pyruvate formate-lyase (PFL: EC 2.3.1.54).[39] Both PFL and B_{12}-**i**GDH require an activating enzyme (PFL-AE or GDH-AE, respectively) to initiate catalysis. The activating enzymes belong to the radical SAM superfamily,[38,40] and thus bind S-adenosylmethionine (SAM) in the vicinity of a [4Fe–4S] cluster. Reductive cleavage of the C–S bond of SAM by the active $[4Fe–4S]^{+1}$ cluster affords Ado• and methionine.[41] The Ado•-carrying GDH-AE (or PFL-AE) may then activate B_{12}-**i**GDH (or PFL) by abstracting an H-atom from a backbone glycine residue (Gly-H) of the primary metabolic enzyme, forming a glycyl radical (Gly•).[42] Once B_{12}-**i**GDH (or PFL) is activated in this way, it may dissociate from GDH-AE (or PFL-AE) and remain active for multiple turnovers.[43] In this dissociated state, the Gly• in B_{12}-**i**GDH (by analogy with PFL) is thought to abstract an H-atom from an

active-site cysteine residue (Cys-H), thus forming Gly-H and Cys•. It is this latter species that is postulated to activate the substrate glycerol (Figure 1).[38,44]

It is noteworthy that despite the generally low sequence and structural similarities between B_{12}-**d**GDH and B_{12}-**i**GDH, and their distinct radical initiators (Ado• and Cys•, respectively), the substrate-binding pockets of the two enzymes are surprisingly similar.[23,38] This has led to suggestions that the two enzymes may represent an example of convergent evolution[6] and share the same substrate mechanism.[38] In contrast to B_{12}-dependent DDH, no ^{18}O-labeling experiments have been performed for B_{12}-**i**GDH so the possible intermediacy of an aldehyde-related radical (A•, Figure 1) cannot be ruled in or out beforehand. Indeed, of the two computational studies on the mechanism of this enzyme, one was performed in the context of the OH-migration mechanism (R• → P•, Figure 1),[45] but it focused on the first H-transfer step, whereas the other concluded that B_{12}-**i**GDH may not involve the migration of a hydroxyl group.[46] In the context of very recent experiments concerned with the isolation and characterization of a B_{12}-independent DDH from *Roseburia inulinivorans* (RiDD or B_{12}-**i**DDH),[47] the possibility of two dehydration mechanisms has been discussed and potentially linked with active site flexibility.

With the goal of advancing the mechanistic understanding of enzymatic glycerol dehydration, this paper presents a comprehensive series of QM/MM calculations focused on the substrate mechanisms of B_{12}-**d**GDH and B_{12}-**i**GDH. We will approach our goal by systematically analyzing aspects of both mechanisms (Figure 1) in both enzymes, all within a single, reliable, methodological framework. Specific emphasis will be placed on the analysis of mechanistic similarities and differences between the two enzymes revealed by such an approach, as well as on rationalizing the reasons underlying their convergent and divergent aspects.

COMPUTATIONAL DETAILS

Small model calculations. The bond dissociation enthalpies (BDEs) shown in Figure 1 were calculated for small model systems at 298.15 K in the gas phase using G3(MP2)-RAD,[48] which has been demonstrated to perform well for the thermodynamic analysis of radical stabilization energies (RSEs) and, to a slightly lesser extent, BDEs.[49] We used methanethiol as an approximation for the BDE for Cys-H, obtaining the value of 361.0 kJ mol^{-1}. In a similar simplification, the adenine ring of Ado-H was replaced by an imidazole group, resulting in a model BDE of 427.9 kJ mol^{-1}. All other BDEs in Figure 1 were calculated for the species as shown. Starting geometries for calculations of R-H, P-H and A-H were taken from conformations that correspond to those in the enzyme environment. Further details are available in Table S1 of the Supporting Information.

Preparation of classical systems. Calculations involving B_{12}-**d**GDH were based upon the PDB structure 1IWP,[23] whereas the PDB structure 1R9D[38] was used for B_{12}-**i**GDH. Protonation states for titratable residues were assigned using H++,[50,51] which accounts for each of the 2^N protonation microstates (when N titratable residues are active).[52] In our calculations, we used the Poisson–Boltzmann formalism, an ionic strength of 0.15 M, an external dielectric constant (ε_{ext}) of 80, an internal dielectric constant (ε_{in}) of 10 and a pH value of 6.5. Because previous studies have revealed the importance of the

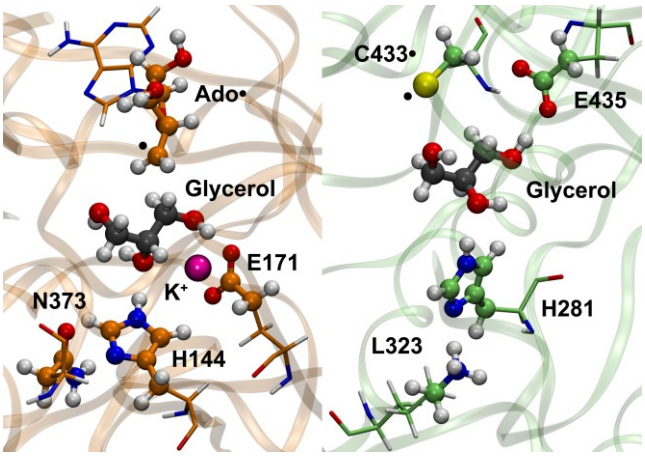

Figure 2. Left: The B_{12}-dependent model system, and Right: The B_{12}-independent model system. The atoms treated quantum-mechanically are shown in a ball-and-stick representation.

protonation states of the histidine residues in the vicinity of the substrate,[29,30,34,36,46] we analyzed these residues more thoroughly (see Table S2). This analysis revealed that His144 of B_{12}-**d**GDH prefers a neutral protonation state (HIE, with the single proton on N_ε), irrespective of the inclusion of the B_{12} cofactor, the substrate or the crystal water molecules in the pK_a (strictly p$K_{1/2}$) evaluation. By comparison, B_{12}-**i**GDH has two histidine residues in close proximity to the substrate and is, therefore, more complex.[53] Evaluation of the p$K_{1/2}$ values for B_{12}-**i**GDH in the absence of the substrate and the crystallographic waters revealed a preference for a neutral His281 (HIE) and a protonated (HIP) His164, in agreement with the previous analysis performed by Feliks et al.[46] However, inclusion of the substrate and/or the crystallographic waters in the computational titrations introduced a large shift in the p$K_{1/2}$ value of His164, showing a strong preference for a neutral state (HID, with the single proton on N_δ). Based on these results, we performed our classical simulations of B_{12}-**i**GDH with the HIE281-HID164 combination, whereas the B_{12}-**d**GDH simulations were performed with HIE144.

After protonation of titratable residues as described above, sodium counterions were used to neutralize the overall charge and the systems were solvated in a truncated octahedron water box using the Amber 9 suite of programs.[54] Valence parameters for cobalamin were obtained from the literature,[55] while RESP charges for AdoCbl were obtained at the IEF-PCM B3LYP/cc-pVTZ level of theory, including the cc-pVTZ-Douglass-Kroll basis set[56] and an atomic radius of 1.80 for Co.[27]

Classical MD simulations. Equilibrations of the systems involved energy minimizations and short (100 ps) MD simulations with systematic decreases to zero of the harmonic restraints and relaxation of the volume and temperature (NPT ensemble) with target values of the temperature and pressure set to 300 K and 1 atm, respectively. For B_{12}-**d**GDH, this resulted in converged density and pressure values of 1.051 ± 0.001 g cm^{-3} and 1.5 ± 46.8 atm, respectively (average ± standard deviation). The snapshot with the instantaneous volume closest to the average volume from the NPT run (density of 1.051 g cm^{-3}, pressure of -13.8 atm for B_{12}-**d**GDH) was chosen for subsequent MD simulations at constant volume (NVT ensemble) at 300 K for a total of 11 ns for each protein. The final 10 ns of these data (T = 300.0 ± 0.7 K for B_{12}-

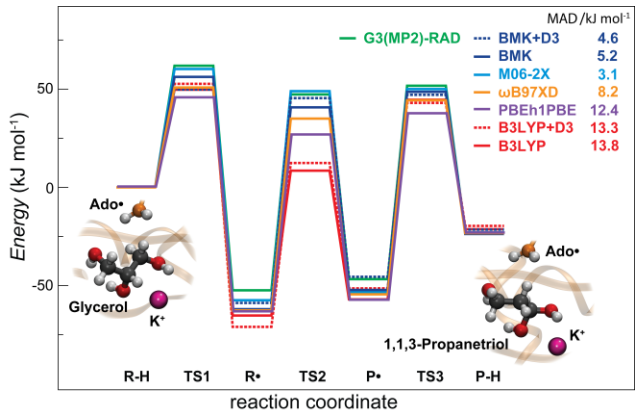

Figure 3. QM/MM benchmark (ONIOM[G3(MP2-RAD):AMBER] and DFT (ONIOM[*F*/6-311+G(3df,2p):AMBER], where *F* = BMK, BMK(+D3), M06-2X, B3LYP(+D3), ωB97XD and PBEh1PBE) results. The model system is described in the Computational Details section.

dGDH) were used to obtain structures for the subsequent QM/MM calculations by taking the structure with the lowest RMSD from the average structure over this time period. The numerical indicators of the equilibration protocol for B_{12}-**i**GDH were essentially identical to those given for B_{12}-**d**GDH. All subsequent QM/MM calculations were based on these equilibrated systems.

QM/MM calculations. All QM/MM calculations were performed with the electrostatic embedding implementation of ONIOM as found in the Gaussian03[57] and, to a lesser extent, the Gaussian09[58] suites of programs. All QM/MM geometries were optimized at the ONIOM[B3LYP/6-31G(d):AMBER] level of theory. Local minima and transition structures were verified as such by evaluating their corresponding Hessian matrices. The topological connectivity of all transition structures was verified by optimizing structures resulting from manual displacements along the Hessian eigenvector associated with the imaginary frequency, in both the forward and reverse directions.

For the B_{12}-independent B_{12}-**i**GDH system, the Antechamber utility of AMBER was used to extract all residues partially within 44.0 Å of the center of mass (COM) of the glycerol molecule. Within this molecular fragment, all atoms within 11.0 Å of glycerol's COM were allowed to move freely in the QM/MM calculations, while the remaining layer of 33.0 Å was fixed to account for long-range electrostatic effects and to provide rigidity to the system. The QM region included glycerol and relevant portions of Cys433 (initially as Cys•), Glu435, His281 and Lys323 (see Figure 2).

A similarly sized, freely moving subset of atoms within 11.0 Å of glycerol's COM was used for the B_{12}-dependent B_{12}-**d**GDH system, though a 38.0 Å residue-based cut-off from glycerol was extracted from the entire equilibrated periodic system. The QM region for B_{12}-**d**GDH included glycerol, K^+, and relevant portions of Ado• (ribose), Glu171, His144 and Asn373 (see Figure 2).

The systems shown in Figure 2 were used for the comparative mechanistic investigation of glycerol dehydration presented herein. The QM systems were thus chosen to include the substrate, the most important proximate amino acids, and the key part of the radical initiator (Cys• or Ado•). Systems of this size are most efficiently treated using density functional theory (DFT). Such a choice, however, carries with it the question of an appropriate functional. In the present work, we directly addressed this issue by performing benchmark QM/MM calculations using the compound ONIOM[G3(MP2-RAD):AMBER] procedure.[59] Selected functionals (*F*) were then tested by evaluating ONIOM[*F*/6-311+G(3df,2p):AMBER] energies (where *F* = BMK,[60] BMK+D3, M06-2X,[61] B3LYP,[62] B3LYP+D3, ωB97XD,[63] and PBEh1PBE,[64] where "+D3" indicates the explicit inclusion of Grimme's D3 atom-pair-wise dispersion correction[65]) and comparing them with the benchmark values. This choice of functionals was partially guided by a recent benchmark study we performed on a range of B_{12}-related H-transfer reactions.[66] Based on our previous experience, we chose not to use examples of pure GGA and meta GGA functionals and focused instead on examples of global hybrid GGA functionals (B3LYP and PBEh1PBE), a range-separated functional with inbuilt dispersion correction (ωB97XD), as well as an example of a meta hybrid functional (BMK). Because we had been interested in the explicit effect of atom-pair-wise dispersion corrections in the QM/MM context, we had initially decided not to employ examples of the Minnesota meta family[67] as these functionals already implicitly cover medium-range dispersion effects due to their parametrization. However, because of its widespread use, we subsequently added M06-2X to the group of tested functionals. For the purpose of the assessment study we used the B_{12}-**d**GDH system (Figure 2, left) with the QM system reduced to only glycerol, K^+ and the methylene group from Ado•. All presented QM/MM energies were calculated at 0 K and include a scaled (by 0.9826)[68] zero-point vibrational energy correction.

RESULTS AND DISCUSSION

Benchmark calculations. To ascertain which density functional was likely to describe the energetics of the enzyme-catalyzed glycerol dehydration most satisfactorily, we characterized the transformation of R-H to P-H, via R• and P• (see Figure 1) for B_{12}-**d**GDH using a minimalistic QM region. The individual steps of glycerol dehydration will be discussed in more detail below in the context of calculations with the larger QM region (Figure 2).

The reference ONIOM[G3(MP2-RAD):AMBER] energy profile, obtained using ONIOM[B3LYP/6-31G(d):AMBER] geometries, is depicted in Figure 3 in green and shows the corresponding energies of the stationary points relative to R-H. As seen, all tested functionals (using the same geometries) agree well with the benchmark value in terms of the relative energy of P-H. The relative energies of the radical intermediates (R• and P•) show somewhat larger deviations, with the majority of functionals apparently over-stabilizing the radicals. Similar trends are observed in the H-transfer transition structures (TS1 and TS3), where the TS energies are underestimated (to varying extents) by all functionals. The largest discrepancies occur for the hydroxyl migration transition structure (TS2). Particularly notable in this respect is the failure of B3LYP, irrespective of the inclusion of dispersion corrections in the QM zone.

The overall performance of the tested functionals can be best gauged by inspecting their mean absolute deviations (MADs in the inset of Figure 3) from the benchmark calculations (numerical values for all stationary points are provided in Table S3 of the Supporting Information). B3LYP (with or without dispersion corrections) is clearly associated with the

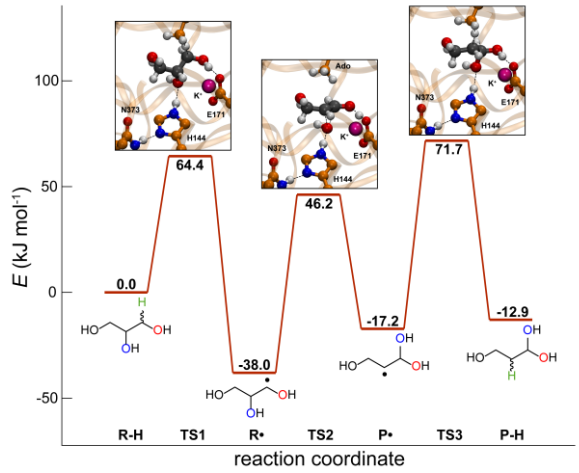

Figure 4. QM/MM results for B_{12}-dependent GDH, showing OH migration with a neutral histidine (B_{12}-**d**GDH, HIE144). The model system is described in the Computational Details section and shown schematically in the left panel of Figure 2. The energies were evaluated with ONIOM[BMK+D3/6-311+G(3df,2p):AMBER].

poorest overall performance (MAD = 13.8 and 13.3 kJ mol^{-1}, respectively). This is a particularly relevant observation as all previous QM/MM studies on diol dehydration[22,34,36,46] have relied heavily on B3LYP as the QM method of choice. PBEh1PBE fares only marginally better with an MAD of 12.4 kJ mol^{-1} and is not recommended for use with reactions of the type shown in Figure 1. ωB97XD, with an MAD of 8.2 kJ mol^{-1}, is certainly preferable to either of the aforementioned functionals but it still underestimates the energy of TS2 by more than 10 kJ mol^{-1} (see Table S3). Notably, the MAD of BMK (5.2 kJ mol^{-1}) essentially falls within chemical accuracy. Its performance is slightly improved by the addition of an empirical dispersion correction, with a resultant MAD of 4.6 kJ mol^{-1}. On this basis, we believe that ONIOM[BMK+D3/6-311+G(3df,2p):AMBER] should prove to be a reliable model chemistry for the investigation of enzyme-catalyzed glycerol dehydration. The remaining energy comparisons presented in this work are made, therefore, using this level of theory. Inspection of Figure 3 and Table S3 shows that M06-2X is associated with a slightly lower MAD (3.1 kJ mol^{-1}) than BMK-D3. For comparison, therefore, we have provided the energies for all profiles with ONIOM[M06-2X/6-311+G(3df,2p):AMBER] in Tables S4-S8. The two functionals provide similar overall results and lead to identical mechanistic conclusions.

Despite the fact that the energies produced by the B3LYP functional are less than ideal, this is not expected to adversely affect the quality of the B3LYP geometries. Namely, geometry is a property that has been established to be much less sensitive to the electronic structure method than the corresponding energy, even in the case of radical reactions.[69]

B_{12}-dependent GDH. In the reaction catalyzed by B_{12}-**d**GDH the first step involves hydrogen-atom abstraction from the substrate (R-H) by 5′-deoxyadenosyl radical (Ado•) to form the closed-shell 5′-deoxyadenosine (Ado-H) and the substrate-derived radical (R•). According to Figure 1, this reaction should be inherently exothermic by 26.6 kJ mol^{-1}. The initial hydrogen-atom abstraction is thought to be followed by migration of the hydroxyl group from the C2 atom to the C1 atom of glycerol to generate the product-related radical (P•) in a mechanistic step that, in the absence of catalysis, would be expected to be associated with very high energy demands (> 100 kJ mol^{-1}).[33] Following OH migration, H-atom re-abstraction from Ado-H by P• may occur to form the closed-shell product (P-H) and regenerate Ado•. On the basis of the BDEs shown in Figure 1, this hydrogen transfer should be very mildly endothermic (2.2 kJ mol^{-1}). The final step of such a mechanism would be the dehydration of P-H to generate the final product aldehyde (A-H).

As shown in Figure 1, there exists a simpler mechanistic possibility involving the dehydration of the radical intermediate R• to give a stabilized radical A•. For A• to be transformed to product, however, it would need to extract a non-activated hydrogen atom from the methyl group of Ado-H. According to the BDE data in Figure 1, this step would be endothermic by 41.7 kJ mol^{-1}, rendering it relatively unlikely. The significantly more facile H-transfer in the first mechanism (from P-H to Ado•) is widely accepted to explain why the 1,2-OH shift occurs. However, such migrations are known to be high in energy,[29] and must therefore benefit from catalysis by the enzyme.

Figure 4 shows the QM/MM energy profile of the transformation of R-H into P-H in the presence of B_{12}-**d**GDH. Using the model chemistry established in the previous section, the first hydrogen-atom transfer is associated with a barrier of 64.4 kJ mol^{-1} (TS1) and it is somewhat more exothermic in the enzyme than would be expected based only upon the BDEs shown in Figure 1. The second step, which involves the transformation of R• into P• by means of a 1,2-OH migration (TS2), is associated with a transition structure that is considerably lower in energy than the one corresponding to H-transfer. The catalytic effect that reduces the barrier of this difficult step has been rationalized by small model calculations[29] and QM/MM calculations on B_{12}-**d**DDH[34] as a synergistic push–pull effect involving His144 (to O2) and Glu171 (from O1, see Figures 2 and 4), with the exact role of the mandatory cation the subject of some discussion.[29,34,70] The final H-transfer (TS3), from Ado-H to R•, is predicted to be rate limiting and, in line with the BDE analysis, is essentially thermoneutral.

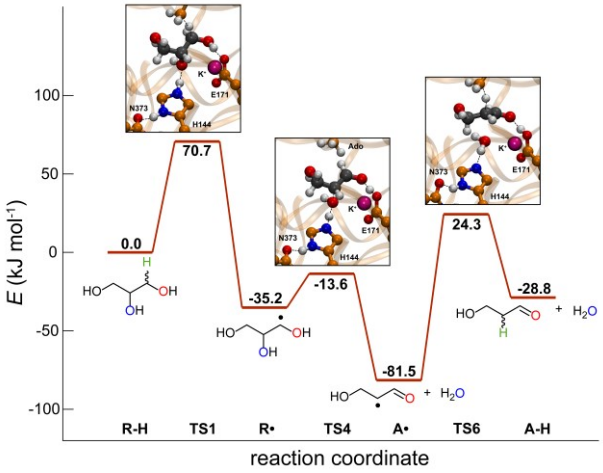

Figure 6. QM/MM results for B_{12}-dependent GDH, showing H_2O elimination with a protonated histidine (B_{12}-**d**GDH, HIP144, H_2O elimination). The model system is analogous to that described in the Computational Details section and shown schematically in the left panel of Figure 2. The energies were evaluated with ONIOM[BMK+D3/6-311+G(3df,2p):AMBER].

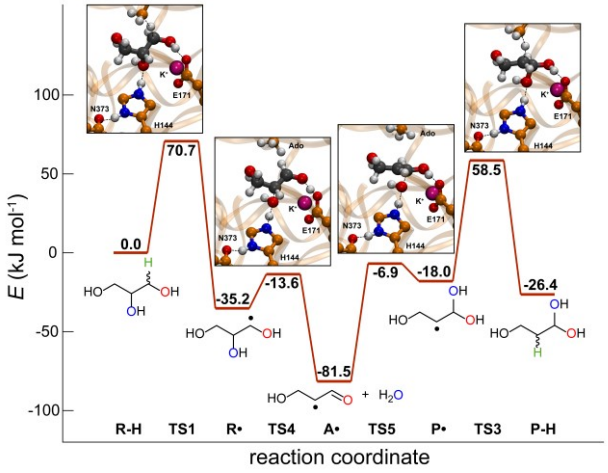

Figure 5. QM/MM results for B_{12}-dependent GDH, showing OH(H) migration with a protonated histidine (B_{12}-**d**GDH, HIP144, OH(H) migration). The model system is analogous to that described in the Computational Details section and shown schematically in the left panel of Figure 2. The energies were evaluated with ONIOM[BMK+D3/6-311+G(3df,2p):AMBER].

A comparison of Figures 3 and 4 leads to the interesting conclusion that, for this particular reaction, the reduced QM system appears to be sufficiently large. We suggest, however, that it is unwise to generalize this conclusion too widely. An intriguing aspect of both profiles (Figures 3 and 4) concerns the relative energies of R• and P•. In isolation, P• is calculated to be more stable than R• by more than 10 kJ mol^{-1},[33] which is consistent with the analogous energy comparison within the ethane-1,2-diol system (where the analog of P• is favored by more than 20 kJ mol^{-1}).[29] The same preference (analogous to E(P•) < E(R•)) is present in almost all of the relevant QM/MM calculations of the propane-1,2-diol system bound to B_{12}-**d**DDH.[34,36] However, this preference is inconsistent with the EPR observation of the 1,2-propanediol-1-yl radical (analog of R•) as the dominant (and hence lowest energy) organic radical in functioning B_{12}-**d**DDH.[31] In contrast, the QM/MM calculations presented in Figures 3 and 4 exhibit a clear preferential stabilization of R• by the enzyme. This stabilization is not only apparent through the reversal of the relative energies of R• and P• but can also be seen by recalling that the initial H-transfer reaction was expected to be exothermic by only 26.6 kJ mol^{-1} (on the basis of BDEs) while the QM/MM results show values at least 11 kJ mol^{-1} larger than this. The experimental observations[31] would therefore suggest that an analogous stabilization is present for B_{12}-**d**DDH and propane-1,2-diol but that the previous QM/MM calculations[34,36] have been unable to capture the effect.

Based on the results of previous small-model calculations,[29] it is of interest to consider the hypothetical mechanism in which His144 in B_{12}-**d**GDH is protonated, even though an analogous mechanism has been previously investigated for B_{12}-**d**DDH with propane-1,2-diol.[34a] The results from the B_{12}-**d**GDH system are shown in Figure 5. Therein, it can be seen that while this small change has a minimal effect on the initial hydrogen abstraction, it has rather drastic consequences for the subsequent steps. Namely, the protonated histidine can be seen to spontaneously transfer its excess proton to the migrating OH group, effectively causing the dehydration of R• (to A• + H_2O) as shown in the alternative pathway in Figure 1 (TS4). It is theoretically possible for the eliminated water to add back at the adjacent carbon (TS5, see Figure 1), to give the same outcome as shown in Figure 4. However, Figure 5 shows that the aldehyde radical (A•) lies in a very deep potential well. If such a well were to be accessed, it would likely result in enzyme inactivation.[33] Nevertheless, if the P• radical were somehow to be formed by water re-addition, it can be seen that the hydrogen transfer to generate P-H would be associated with much the same energetic demands as in the model shown in Figure 4 with a non-protonated His144.

Additional calculations shown in Figure 6 show that direct hydrogen transfer from the methyl group of Ado-H to the stable aldehyde radical (A•, analogous to the upper pathway in Figure 1) is endothermic by 52.7 kJ mol^{-1} and associated with a barrier (TS6) of 105.8 kJ mol^{-1}. This result strongly reinforces the conclusion that full protonation of the migrating oxygen would be very likely to result in deactivation of B_{12}-**d**GDH.

Given the potentially deleterious effect of the protonating His144, it is tempting to speculate that one of the roles played by the substrate-binding cation is actually to suppress the side-chain pK_a of His144 and prevent it from becoming protonated. Some circumstantial evidence for such a speculation can be found by considering the mechanism of B_{12}-**i**GDH, as presented in the following section.

B_{12}-independent GDH. As mentioned previously, the B_{12}-**i**GDH is isofunctional with B_{12}-**d**GDH even though the two enzymes exhibit no significant sequence or structural homology with one another. Interestingly, however, their active sites (Figure 2) are very similar. Apart from the occurrence of a similar pattern of hydrophobic residues close to the radical initiator, the pattern of their polar residues is also very similar. In particular, the "migrating" oxygen (O2) of the substrate is close to a histidine residue in both cases, whereas the adjacent "spectator" oxygen (O1) is in close contact with a glutamate residue in both enzymes.

As mentioned in the Computational Details section, there is an additional histidine residue (His164) close to the substrate in B_{12}-**i**GDH. A previous computational investigation of the mechanism of this enzyme was performed with this residue in its protonated form (HIP164).[46] In the light of the results in Figures 5 and 6, it is perhaps not surprising that HIP164 played a pivotal role in the previously reported mechanism.[46] However, our own p$K_{1/2}$ calculations indicate that this residue has a strong preference for neutrality in the presence of the substrate and crystallographic waters (Table S2); our mechanistic investigations were thus performed with this residue in a neutral state (HID164).

An intriguing difference between the active sites of the two enzymes concerns the requirement of a potassium ion for the function of B_{12}-**d**GDH but not for B_{12}-**i**GDH. It is noteworthy that, even with His164 in its neutral form, another positive charge is present near the substrate of B_{12}-**i**GDH. This comes in the form of (protonated) Lys323, which can be found on the rear side of the His281 (Figure 2). Nevertheless, the most important difference between the two enzymes likely concerns the radical activation of the substrate. Namely, B_{12}-**i**GDH has its radical chemistry initiated by a sulfur-based thiyl radical from a cysteine residue, as opposed to the carbon-based Ado• utilized by B_{12}-**d**GDH.

As shown in Figure 1, the S–H BDE of a cysteine residue is calculated to be around 361.0 kJ mol^{-1}, which is considerably lower than the C–H BDE of Ado-H (427.9 kJ mol^{-1}). This implies that the activation of the substrate R-H (BDE = 401.3 kJ mol^{-1}) by Cys• should be intrinsically endothermic by some 40.3 kJ mol^{-1}. If the 1,2-OH migration were to proceed as in the B_{12}-**d**GDH mechanism (via R• and P•), one could expect the final H-transfer from an intact cysteine (Cys-H) to the P• radical (P-H BDE = 425.7 kJ mol^{-1}) to be exothermic by some 64.7 kJ mol^{-1}.

A mechanistic profile (via R• and P•) for B_{12}-**i**GDH obtained by our QM/MM approach is shown in Figure 7. It can be seen that, like B_{12}-**d**GDH, B_{12}-**i**GDH preferentially stabilizes the R• intermediate. Once again, this is evident through either the fact that (enzyme-bound) R• is significantly more stable than (enzyme-bound) P• or the fact that the intrinsic endothermicity of the initial H-transfer (40.3 kJ mol^{-1} on the basis of BDEs) has been substantially reduced (to 17.6 kJ mol^{-1}) in the presence of B_{12}-**i**GDH. The barrier for the initial H-transfer reaction is also significantly lower for B_{12}-**i**GDH than for B_{12}-**d**GDH. However, this is more likely to be related to the facility of H-transfers between S and C atoms (relative to that between two C atoms) rather than any additional transition-structure stabilization (of TS1) by the enzyme. Overall, the results imply that the activation of R-H by Cys• in the presence of B_{12}-**i**GDH appears to be not only feasible but also facile.

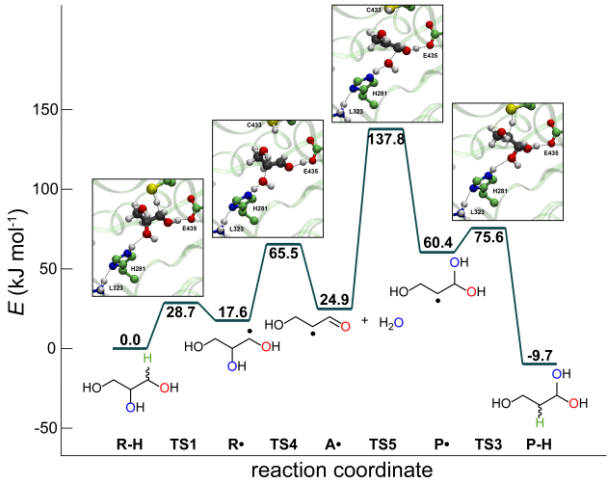

Figure 7. QM/MM results for B_{12}-independent GDH, showing OH(H) migration (B_{12}-**i**GDH, OH(H) migration). The model system is described in the Computational Details section and shown schematically in the right panel of Figure 2. The energies were evaluated with ONIOM[BMK+D3/6-311+G(3df,2p):AMBER].

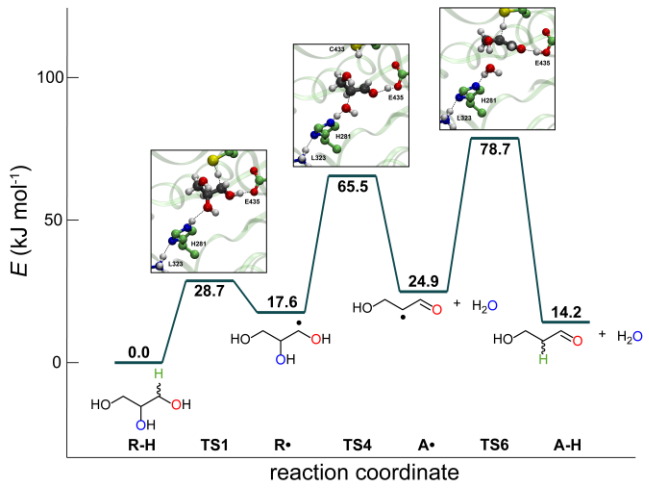

Figure 8. QM/MM results for B_{12}-independent GDH, showing H_2O elimination (B_{12}-**i**GDH, H_2O elimination). The model system is described in the Computational Details section and shown schematically in the right panel of Figure 2. The energies were evaluated with ONIOM[BMK+D3/6-311+G(3df,2p):AMBER].

Following substrate activation, the mechanism of B_{12}-**i**GDH appears to diverge from that of B_{12}-**d**GDH. Specifically, even though neither His164 nor His281 are initially protonated, the combined absence of the potassium ion and the presence of a protonated Lys323 at the rear side of His281 are sufficient to result in a relayed proton transfer from Lys323 to the "migrating" oxygen of the substrate in B_{12}-**i**GDH (see Figure 7). This is similar yet clearly different to the mechanism involving direct substrate protonation by HIP144 in B_{12}-**d**GDH shown in Figure 5 (or, for that matter, direct substrate protonation by HIP164, as previously reported for B_{12}-**i**GDH[46]). However, inspection of Figure 7 shows that, in the case of B_{12}-**i**GDH, the aldehyde radical (A•) is not particularly stabilized relative to the remaining radical intermediates of the dehydration mechanism (in contrast to Figure 5). Indeed, it is predicted to be slightly higher in energy than the reactant radical R•. In principle, this could imply that the re-addition of the water molecule to the adjacent carbon atom (TS5) is more feasible than for the protonated mechanism of B_{12}-**d**GDH (Figure 5). However, inspection of Figure 7 reveals that in practice this is unlikely, with the calculated barrier for the formation of the P• radical (from A•) amounting to 112.9 kJ mol^{-1} (TS5). In accordance with expectations based on the BDE analysis, the H-transfer from cysteine to the P• radical (if it were to be formed) would be facile and exothermic by 70.1 kJ mol^{-1}.

On the basis of the above calculations, it seems that the mechanism involving a 1,2-OH shift (by way of the elimination (TS4) and re-addition (TS5) of a water molecule) is not a viable mechanism for B_{12}-**i**GDH. In the context of the mechanistic scenarios shown in Figure 1, it is of interest to consider the ability of the aldehyde radical (A•) to abstract an H-atom from an intact cysteine residue (Cys-H). Based on the BDE considerations apparent from Figure 1, such a transfer should actually be exothermic by 25.2 kJ mol^{-1}.

The QM/MM profile of the upper mechanism of Figure 1 for B_{12}-**i**GDH is displayed in Figure 8. The first two steps, in which the substrate is activated (TS1) and the resulting radical eliminates water (TS4), are identical to those shown in Figure 7 (involving the proton relay). In Figure 8, however, the aldehyde radical (A•) abstracts an H-atom from Cys433 (TS6). Although the exothermicity of this step is somewhat reduced from the simple BDE-based estimate, this step seems both kinetically ($\Delta H^{\ddagger}$ = 53.8 kJ mol^{-1}) and thermodynamically (ΔH = −10.7 kJ mol^{-1}) viable. Indeed, when compared with the (radical rearrangement) mechanism shown in Figure 7, it is relatively clear that the elimination/abstraction scenario depicted in Figure 8 is significantly more favorable.

For both B_{12}-**d**GDH and B_{12}-**i**GDH, a mechanism involving the elimination of water from the substrate-derived radical (R•) requires the presence of an acidic proton. When this proton is manually introduced at His144 of B_{12}-**d**GDH, despite the indications of p$K_{1/2}$ values to the contrary, H_2O elimination (TS4) becomes mechanistically dominant, albeit unproductive (see Figures 5 and 6 and reference 34a). In this context, the previous finding that manually protonating His164 of B_{12}-**i**GDH resulted in H_2O elimination[46] is perhaps not overly surprising. Nor can it really be considered sufficient to prove the operability of the elimination mechanism in B_{12}-**i**GDH. However, the observation that elimination still occurs in B_{12}-**i**GDH, even when both proximate histidine residues (164 and 281) are neutral (in accordance with p$K_{1/2}$ calculations, Table S2), is a rather convincing result. Placed properly in the overall context of calculations of both mechanisms for both enzymes on an equal and reliable footing, and combining this information with appropriate thermodynamic considerations, it seems possible to draw some solid conclusions regarding the enzymatic dehydration of glycerol.

CONCLUSIONS

In summary, we have used a QM/MM approach to investigate, compare and contrast the mechanism of glycerol dehydration in the presence of two isofunctional enzymes, B_{12}-dependent (B_{12}-**d**GDH) and B_{12}-independent (B_{12}-**i**GDH) glycerol dehydratases. Despite the fact that these two enzymes bear virtually no sequential or structural similarity to one another, they have remarkably similar substrate binding sites. Nevertheless, it appears that the subtle differences between these active sites result in markedly different dehydration mechanisms. The differences in these mechanisms seem to be strongly related, on the one hand, to the X–H bond strength of the radical initiator and, on the other hand, to the protonation environment of the "migrating" oxygen of the substrate. It appears also that no special invocation of active-site flexibility is required to rationalize the appearance of two dehydration mechanisms.

When the radical initiator has a high X–H bond strength, as in the case of B_{12}-**d**GDH (C–H BDE of 427.9 kJ mol^{-1}), a mechanism involving a 1,2-OH shift is strongly preferred (Figure 4). The driving force for such a mechanism can be found in a thermodynamic mismatch of BDEs in the alternative radical elimination mechanism (Figure 1, upper pathway). That is, the resonance stability present in the aldehyde radical intermediate (A•) makes it unlikely that the 386.2 kJ mol^{-1} gained from forming the missing C–H bond is sufficient to counterbalance the 427.9 kJ mol^{-1} required to cleave the C–H bond of Ado-H. Seemingly in response to this energy mismatch, the enzyme offers significant catalytic assistance to the ordinarily difficult 1,2-migration of an OH group. Completing this step implies that the C–H bond formed (in P-H) upon abstracting an H-atom supplies some 425.7 kJ mol^{-1}, which is a much better match for the 427.9 kJ mol^{-1} contained in the Ado-H bond.

That the balance between catalysis and catastrophe is delicate is nicely demonstrated by considering the mechanism of B_{12}-**d**GDH when His144 is protonated. This small change forces the elimination of water from the R• radical forming the stabilized aldehyde radical intermediate (A•, Figure 5). Not only is the H abstraction from 5'-deoxyadenosine by this intermediate energetically unfavorable, so too is the re-addition of water and the formation of the more reactive P• intermediate (which would allow a more facile H abstraction). This combination strongly implies that the enzyme must control the protonation state of His144 such that catalysis of the 1,2-OH shift is enabled but inactivation is avoided. It is tempting to speculate in this respect that part of the role played by the requisite cation is to suppress the pK_a of His144 and aid in this control.

When the radical initiator has a low X–H bond strength, as in the case of B_{12}-**i**GDH (S–H BDE of 361.0 kJ mol^{-1}), the situation is effectively reversed. In this case protonation of the migrating oxygen need not be avoided because of a thermodynamic mismatch; the 386.2 kJ mol^{-1} gained from forming the missing C–H bond in the aldehyde-related radical (A•) is more than sufficient to effect the cleavage of the S–H bond (which requires only 361.0 kJ mol^{-1}). The OH(H) migration pathway that would lead to an intermediate with a significantly higher BDE is neither required nor accessible. Significantly, this mechanism would predict that the scrambling of ^{18}O labels, which occurred in the dehydration of ^{18}O-labelled propane-1,2-diols with B_{12}-**d**DDH, would *not* be observed. In addition, seemingly in response to the balanced thermodynamics of the H-transfer, the structure of the active site is such that the enzyme is poised to carry out the (indirect) protonation of the migrating oxygen, ensuring the dehydration and primacy of the more economical mechanism.

ASSOCIATED CONTENT

Supporting Information. Supplementary Figures S1 to S6 and Supplementary Tables S1 to S9. This material is available free of charge via the Internet at http://pubs.acs.org.

AUTHOR INFORMATION

Corresponding Author. David.Smith@irb.hr

ACKNOWLEDGMENTS

This work was financially supported by the Croatian Science Foundation project CompSoLS-MolFlex (IP-11-2013-8238). The computational resources were provided by the University Computing Centre (SRCE), the University of Zagreb and the Croatian National Grid Infrastructure (CRO-NGI).

REFERENCES

(1) (a) Toraya, T. *Cell. Mol. Life Sci.* **2000**, *57*, 106–127. (b) Toraya, T. *Chem. Rev.* **2003**, *103*, 2095–2127.

(2) (a) Smiley, K. L.; Sobolov, M. *Arch. Biochem. Biophys.* **1962**, *97*, 538–543. (b) Pawelkiewicz, J.; Zagalak, B. *Acta Biochim. Polon.* **1965**, *12*, 207–218.

(3) Abeles, R. H.; Brownstein, A. M.; Randles, C. H. *Biochim. Biophys. Acta.* **1960**, *41*, 530–531.

(4) (a) Toraya, T.; Fukui, S. *Eur. J. Biochem.* **1977**, *76*, 285–289. (b) Toraya, T.; Kuno, S.; Fukui, S. *J. Bacteriol.* **1980**, *141*, 1439–1442. (c) Forage, R. G.; Foster, M. A. *Biochim. Biophys. Acta* **1979**, *569*, 249–258.

(5) Veiga-da-Cunha, M.; Foster, M. A. *Appl. Environ. Microbiol.* **1992**, *58*, 2005–2010.

(6) Liu, J.-Z.; Xu, W.; Chistoserdov, A.; Bajpai, R. K. *Appl. Biochem. Biotechnol.* **2016**, *179*, 1073–1100.

(7) Thompson, J. C.; He, B. B. *Appl. Eng. Agric.* **2006**, *22*, 261–265.

(8) Aldiguier, A. S.; Alfenore, S.; Cameleyre, X.; Goma, G.; Uribelarrea, J. L.; Guillouet, S. E.; Molina-Jouve, C. *Bioprocess Biosyst. Eng.* **2004**, *26*, 217–222.

(9) (a) Yazdani, S. S.; Gonzalez, R. *Curr. Opin. Biotech.* **2007**, *18*, 213–219. (b) Clomburg, J. M.; Gonzalez, R. *Trends Biotechnol.* **2013**, *31*, 20–28.

(10) Chen, Z.; Liu, D. *Biotechnol Biofuels* **2016**, *9*, 205.

(11) Vollenweider, S.; Lacroix, C. *Appl. Microbiol. Biotechnol.* **2004**, *64*, 16–27.

(12) Bauer, R.; Cowan, D. A.; Crouch, A. *J Agric. Food Chem.* **2010**, *58*, 3243–3250.

(13) Oehmke, S.; Zeng, A.-P. *Eng. Life Sci.* **2015**, *15*, 133–139.

(14) Jiang, W.; Wang, S.; Wang, Y.; Fang, B. *Biotechnol. Biofuels*, **2016**, *9*, 57.

(15) Liu, H.; Xu, Y.; Zheng, Z.; Liu, D. *Biotechnol. J.* **2010**, *5*, 1137–1148.

(16) Jun, S. A.; Moon, C.; Kang, C. H.; Kong, S. W.; Sang, B. I.; Um, Y. *Appl. Biochem. Biotechnol.* **2010**, *161*, 1–8.

(17) (a) Kraus, G. A. *CLEAN – Soil, Air, Water*, **2008**, *36*, 648–651. (b) Huang, H.; Gong, C. S.; Tsao, G. T. *Appl. Microbiol. Biotechnol.* **2002**, *98–100*, 687–698.

(18) (a) Rossi, D. M.; de Souza, E. A.; Flores, S. H.; Ayub, M. A. Z. *Renew. Energy* **2012**, *39*, 223–227. (b) Qi, X.; Guo, Q.; Wei, Y.; Xu, H.; Huang, R. *Biotechnol. Lett.* **2012**, *34*, 339– 346. (c) de Souza, E. A.; Rossi, D. M.; Ayub, M. A. Z. *Renew. Energy* **2014**, *72*, 253–257. (d) Pflügl, S.; Marx, H.; Mattanovich, D.; Sauer, M. *Bioresour. Technol.*, **2014**, *152*, 499–504. (e) Durgapal, M.; Kumar, V.; Yang, T. H.; Lee, H. J.; Seung, D.; Park, S. *Bioresour. Technol.*, **2014**, 159, 223–231.

(19) (a) Tang, X.; Tan, Y.; Zhu, H.; Zhao, K.; Shen, W. *Appl. Environ. Microbiol.* **2009**, *75*, 1628–1634. (b) Celińska, E. *Biotechnol. Adv.* **2010**, *28*, 519–530.

(20) Toraya, T. *Arch. Biochem. Biophys.* **2014**, *544*, 40–57.

(21) (a) Toraya, T. *Metal Ions Biol. Sys.* **1994**, *30*, 217–254. (b) Toraya, T. In Banerjee, R., Ed. Chemistry and Biochemistry of B_{12}; John Wiley & Sons: New York, 1999.

(22) (a) Kamachi, T.; Takahata, M.; Toraya, T.; Yoshizawa, K. *J. Phys. Chem. B*, **2009**, *113*, 8435–8438. (b) Kamachi, T.; Doitomi, K.; Takahata, M.; Toraya, T.; Yoshizawa, K. *Inorg. Chem.* **2011**, *50*, 2944–2952.

(23) Yamanishi, M.; Yunoki, M.; Tobimatsu, T.; Sato, H.; Matsui, J.; Dokiya, A.; Iuchi, Y.; Oe, K.; Suto, K.; Shibata, N.; Morimoto, Y.; Yasuoka, N.; Toraya, T. *Eur. J. Biochem.* **2002**, *269*, 4484–4494.

(24) (a) Shibata, N.; Masuda, J.; Tobimatsu, T.; Toraya, T.; Suto, K.; Morimoto, Y.; Yasuoka, N. *Structure*, **1999**, *7*, 997–1008. (b) Masuda, J.; Shibata, N.; Morimoto, Y.; Toraya, T.; Yasuoka, N. *Structure*, **2000**, *8*, 775–788.

(25) Banerjee, R., Ed. Chemistry and Biochemistry of B_{12}; John Wiley & Sons: New York, 1999.

(26) Sandala, G. M.; Smith, D. M.; Radom, L. *Acc. Chem. Res.* **2010**, *43*, 642–651.

(27) Bucher, D.; Sandala; G. M.; Durbeej, B.; Radom, L.; Smith, D. M. *J. Am. Chem. Soc.* **2012**, *134*, 1591–1599.

(28) (a) Anderson, R. J.; Ashwell, S.; Dixon, R. M.; Golding, B. T. *J. Chem. Soc., Chem. Commun.* **1990**, 70–72. (b) Retey, J.; Umani-Ronchi, A.; Arigoni, D. *Experientia* **1966**, *22*, 72–73. (c) Rétey, J.; Umani-Ronchi, A.; Seibl, J.; Arigoni, D. *Experientia* **1966**, *22*, 502.

(29) (a) Smith, D. M.; Golding, B. T.; Radom, L. *J. Am. Chem. Soc.* **1999**, *121*, 5700–5704. (b) Smith, D. M.; Golding, B. T.; Radom, L. *J. Am. Chem. Soc.* **2001**, *123*, 1664–1675.

(30) (a) Golding, B. T.; Radom, L. *J. Chem. Soc., Chem. Commun.* **1973**, 939–941. (b) Golding, B. T.; Radom, L. *J. Am. Chem. Soc.* **1976**, *98*, 6331–6338.

(31) Yamanishi, M.; Ide, H.; Murakami, Y.; Toraya, T.; *Biochemistry* **2005**, *44*, 2113–2118.

(32) Pierik, A. J.; Graf, T.; Pemberton, L.; Golding, B. T.; Rétey, J. *ChemBioChem* **2008**, *9*, 2268–2275.

(33) Sandala, G. M., Kovačević, B., Barić, D., Smith, D. M.; Radom, L. *Chem. Eur. J.* **2009**, *15*, 4865–4873.

(34) (a) Kamachi, T.; Toraya, T.; Yoshizawa, K. *J. Am. Chem. Soc.* **2004**, *126*, 16207–16216. (b) Doitomi, K.; Kamachi, T.; Toraya, T.; Yoshizawa, K. *Biochemistry* **2012**, *51*, 9202−9210.

(35) (a) Kawata, M.; Kinoshita, K.; Takahashi, S.; Ogura, K.; Komoto, N.; Yamanishi, M.; Tobimatsu, T.; Toraya, T. *J. Biol. Chem.* **2006***, 281,* 18327–18334*.* (b) Kinoshita, K.; Kawata, M.; Ogura, K.; Yamasaki, A.; Watanabe, T.; Komoto, N.; Hieda, N.; Yamanishi, M.; Tobimatsu, T.; Toraya, T. *Biochemistry* **2008**, *47*, 3162–3173. (c) Yamanishi, M.; Kinoshita, K.; Fukuoka, M.; Saito, T.; Tanokuchi, A.; Ikeda, Z.; Obayashi, H.; Mori, K.; Shibata, N.; Tobimatsu, T.; Toraya, T. *FEBS J.* **2012**, *279*, 793–804.

(36) (a) Kamachi, T.; Toraya, T.; Yoshizawa, K. *Chem. Eur. J.* **2007**, *13*, 7864–7873. (b) Doitomi, K.; Tanaka, H.; Kamachi, T.; Toraya, T.; Yoshizawa, K. *Bull. Chem. Soc. Jpn.* **2014**, *87*, 950–959. (c) Doitomi, K.; Kamachi, T.; Toraya, T.; Yoshizawa, K. *Bull. Chem. Soc. Jpn.* **2016**, *89*, 955–964.

(37) Raynaud, C.; Sarçabal, P.; Meynial-Salles, I.; Croux, C.; Soucaille, P. *Proc. Natl. Acad. Sci. U.S.A*. **2003**, *100*, 5010–5015.

(38) O'Brien, J. R.; Raynaud, C.; Croux, C.; Girbal, L.; Soucaille, P.; Lanzilotta, W. N. *Biochemistry* **2004**, *43*, 4635–4645.

(39) Knappe, J.; Blaschkowski, H. P.; Gröbner, P.; Schmitt, T. *Eur. J. Biochem.* **1974**, *50*, 253–263.

(40) (a) Frey, P. A.; Magnusson O. Th. *Chem. Rev.* **2003**, *103*, 2129–2148. (b) Sofia, H. J.; Chen, G.; Hetzler, B. G.; Reyes-Spindola, J. F; Miller, N. E. *Nucleic Acids Res.* **2001**, *29*, 1097–1106.

(41) Walsby, C. J.; Ortillo, D.; Broderick, W. E.; Broderick, J. B.; Hoffman, B. M. *J. Am. Chem. Soc.* **2002**, *124*, 11270–11271.

(42) (a) Frey, M.; Rothe, M.; Wagner, A. F.; Knappe, J. *J. Biol. Chem.* **1994**, *269*, 12432–12437. (b) Henshaw, T. F.; Cheek, J.; Broderick, J. B. *J. Am. Chem. Soc.* **2000**, *122*, 8331–8332.

(43) Shisler, K. A.; Broderick, J. B. *Arch. Biochem. Biophys.* **2014**, *546*, 64–71.

(44) Parast, C.V.; Wong, K. K.; Lewisch, S. A.; Kozarich, J. W. *Biochemistry* **1995**, *34*, 2392–2399.

(45) (a) Liu, Y.; Gallo, A. A.; Florian, J.; Liu, Y.-S.; Mora, S.; Xu, W. *J. Phys. Chem. B* **2010**, *114*, 5497–5502. (b) Liu, Y.; Gallo, A. A.; Xu, W.; Bajpai, R.; Florian, J. *J. Phys. Chem. A* **2011**, *115*, 11162–11166.

(46) Feliks, M.; Ullmann, G. M. *J. Phys. Chem. B* **2012**, *116*, 7076–7087.

(47) LaMattina, J. W.; Keul, N. D.; Reitzer, P.; Kapoor, S.; Galzerani, F.; Koch, D. J.; Gouvea, I. E.; Lanzilotta, W. N. *J. Biol. Chem.* **2016**, *291*, 15515–15526.

(48) (a) Henry, D. J.; Parkinson, C. J.; Radom, L. *J. Phys. Chem. A*, **2002**, *106*, 7927–7936. (b) Henry, D. J.; Sullivan, M. B.; Radom, L. *J. Chem. Phys.* **2003**, *118*, 4849–4860.

(49) (a) Hioe, J.; Zipse, H. *Faraday Discuss.* **2010**, *145*, 301–313. (b) Hioe, J.; Zipse, H. *Org. Biomol. Chem.*, **2010**, *8*, 3609–3617.

(50) H++: web-based computational prediction of protonation states and pK of ionizable residues in macromolecules: http://biophysics.cs.vt.edu.

(51) Gordon, J. C.; Myers, J. B.; Folta, T.; Shoja, V.; Heath, L. S.; Onufriev, A. *Nucleic Acids Res.* **2005**, *33*, W368-W371.

(52) Anandakrishnan, R.; Onufriev, A. *J. Comp. Biol*. **2008**, *15*, 165–184.

(53) Čondić-Jurkić, K.; Smith, A.-S.; Zipse, H.; Smith, D. M. *J. Chem. Theory Comput.* **2012**, *8*, 1078–1091.

(54) Case, D. A.; Darden, T. A.; Cheatham, T. E., III; Simmerling, C. L.; Wang, J.; Duke, R. E.; Luo, R.; Merz, K. M.; Pearlman, D. A.; Crowley, M.; Walker, R. C.; Zhang, W.; Wang, B.; Hayik, S.; Roitberg, A.; Seabra, G.; Wong, K. F.; Paesani, F.; Wu, X.; Brozell, S.; Tsui, V.; Gohlke, H.; Yang, L.; Tan, C.; Mongan, J.; Hornak, V.; Cui, G.; Beroza, P.; Mathews, D. H.; Schafmeister, C.; Ross, W. S.; Kollman, P. A. AMBER 9, University of California, San Francisco (2006).

(55) Marques, H. M.*;* Ngoma, B.; Egan, T. J.; Brown, K. L. *J. Mol. Struct.* **2001**, *561*, 71–91.

(56) Balabanov, N. B.; Peterson, K. A. *J. Chem. Phys.* **2005**, *123*, 64107.

(57) Frisch, M. J.; Trucks, G. W.; Schlegel, H. B.; Scuseria, G. E.; Robb, M. A.; Cheeseman, J. R.; Montgomery, Jr., J. A.; Vreven, T.; Kudin, K. N.; Burant, J. C.; Millam, J. M.; Iyengar, S. S.; Tomasi, J.; Barone, V.; Mennucci, B.; Cossi, M.; Scalmani, G.; Rega, N.; Petersson, G. A.; Nakatsuji, H.; Hada, M.; Ehara, M.; Toyota, K.; Fukuda, R.; Hasegawa, J.; Ishida, M.; Nakajima, T.; Honda, Y.; Kitao, O.; Nakai, H.; Klene, M.; Li, X.; Knox, J. E.; Hratchian, H. P.; Cross, J. B.; Bakken, V.; Adamo, C.; Jaramillo, J.; Gomperts, R.; Stratmann, R. E.; Yazyev, O.; Austin, A. J.; Cammi, R.; Pomelli, C.; Ochterski, J. W.; Ayala, P. Y.; Morokuma, K.; Voth, G. A.; Salvador, P.; Dannenberg, J. J.; Zakrzewski, V. G.; Dapprich, S.; Daniels, A. D.; Strain, M. C.; Farkas, O.; Malick, D. K.; Rabuck, A. D.; Raghavachari, K.; Foresman, J. B.; Ortiz, J. V.; Cui, Q.; Baboul, A. G.; Clifford, S.; Cioslowski, J.; Stefanov, B. B.; Liu, G.; Liashenko, A.; Piskorz, P.; Komaromi, I.; Martin, R. L.; Fox, D. J.; Keith, T.; Al-Laham, M. A.; Peng, C. Y.; Nanayakkara, A.; Challacombe, M.; Gill, P. M. W.; Johnson, B.; Chen, W.; Wong, M. W.; Gonzalez, C.; Pople, J. A. Gaussian 03, Revision E.01, Gaussian, Inc., Wallingford CT (2004).

(58) Frisch, M. J.; Trucks, G. W.; Schlegel, H. B.; Scuseria, G. E.; Robb, M. A.; Cheeseman, J. R.; Scalmani, G.; Barone, V.;

Petersson, G. A.; Nakatsuji, H.; Li, X.; Caricato, M.; Marenich, A.; Bloino, J.; Janesko, B. G.; Gomperts, R.; Mennucci, B.; Hratchian, H. P.; Ortiz, J. V.; Izmaylov, A. F.; Sonnenberg, J. L.; Williams-Young, D.; Ding, F.; Lipparini, F.; Egidi, F.; Goings, J.; Peng, B.; Petrone, A.; Henderson, T.; Ranasinghe, D.; Zakrzewski, V. G.; Gao, J.; Rega, N.; Zheng, G.; Liang, W.; Hada, M.; Ehara, M.; Toyota, K.; Fukuda, R.; Hasegawa, J.; Ishida, M.; Nakajima, T.; Honda, Y.; Kitao, O.; Nakai, H.; Vreven, T.; Throssell, K.; Montgomery, Jr., J. A.; Peralta, J. E.; Ogliaro, F.; Bearpark, M.; Heyd, J. J.; Brothers, E.; Kudin, K. N.; Staroverov, V. N.; Keith, T.; Kobayashi, R.; Normand, J.; Raghavachari, K.; Rendell, A.; Burant, J. C.; Iyengar, S. S.; Tomasi, J.; Cossi, M.; Millam, J. M.; Klene, M.; Adamo, C.; Cammi, R.; Ochterski, J. W.; Martin, R. L.; Morokuma, K.; Farkas, O.; Foresman, J. B.; Fox D. J. Gaussian 09, Revision A.02, Gaussian, Inc., Wallingford CT (2016).

(59) Čondić-Jurkić, K.; Zipse, H.; Smith, D. M. *J. Comput. Chem.* **2010**, *31*, 1024–1035.

(60) Boese, A. D.; Martin, J. M. L. *J. Chem. Phys.* **2004**, *121*, 3405–3416.

(61) Zhao, Y.; Truhlar, D. *Theor. Chem. Acc.* **2008**, *120*, 215−241.

(62) Becke, A. D. *J. Chem. Phys*. **1993**, *98*, 5648–5652.

(63) Chai, J.-D.; Head-Gordon, M. *Phys. Chem. Chem. Phys.* **2008**, *10*, 6615–6620.

(64) Ernzerhof, M.; Perdew, J. P. *J. Chem. Phys.* **1998**, *109*, 3313–3320.

(65) Grimme, S.; Ehrlich, S.; Goerigk, L. *J. Comput. Chem.* **2011**, *32*, 1456–1465.

(66) Wick, C. R.; Smith, D. M. *J. Phys. Chem. A* **2018**, *122*, 1747–1755.

(67) Peverati, R.; Truhlar, D. G. *Phil. Trans. R. Soc. A* **2014**, *372*, 20120476.

(68) Merrick, J. P.; Moran, D.; Radom, L. *J. Phys. Chem. A* **2007**, *111*, 11683–11700.

(69) Smith, D. M.; Nicolaides, A; Golding, B. T.; Radom, L. *J. Am. Chem. Soc.* **1999**, *120*, 10223–10233.

(70) Toraya, T.; Yoshizawa, K.; Eda, M.; Yamabe, T. *J. Biochem.* **1999**, *126*, 650–654.

TOC GRAPHIC